The Cooper Union for the Advancement of Science and Art

Aerodynamic Analysis of the Boeing B-29 Superfortress

ME-422: Fundamentals of Aerodynamics

Author:
Benjamin Aziel

Professor:
David Wootton

Last Updated: May 10, 2024

Contents

1 Motivation and Overview

This project examines the aerodynamic characteristics of the Boeing B-29 Superfortress, a groundbreaking aircraft that pushed the boundaries of aeronautical engineering during World War II. Its massive size, advanced pressurized cabin, and sophisticated fire control systems were remarkable achievements for the time. The aerodynamic design of the B-29's wing played a crucial role in its performance capabilities.

These unorthodox aerodynamic design of the B-29 make it a rewarding subject to explore in depth for this project. The analysis explores both 2D and 3D effects through a combination of theoretical calculations and computational simulations.

While theoretical "back of the envelope" calculations are valuable, higher-fidelity computational tools like XFLR5 can model the full 3D geometry and validate our hand calculations. These tools provide a more comprehensive analysis of the aerodynamic characteristics.

2 Technical Specifications and Property Assumptions

Specifications for the plane as a whole were available through many sources, including but not limited to the National Museum of the United States Air Force, Nuclear Companion, and of course, Wikipedia (I *am* an engineer after all, aha.)

B-29 Specifications			
Attribute	Symbol	US	Metric
Wingspan	b	141.25 ft	43.05 m
Wing Area	S	1736 ft^2	161.3 m^2
Maximum Takeoff Weight	W_{max}	133500 lbf	593837.37 N
Cruise Speed	V_{cruise}	220 mph	98.35 m/s

A constant twist along the wing of -1° is assumed.

The airfoil profile at the root and tip sections are readily available through Airfoil Tools (here's the root and here's the tip), but I was unable to find data for the chord length at either section. To get around this issue, I looked at a three-view image of the B-29 and used the video analysis tool Tracker to measure the length of each section, using the wingspan as a reference length.

Airfoil Chord Lengths			
Attribute	Symbol	US	Metric
B-29 Root Airfoil	c_{root}	18 ft	5.5 m
B-29 Tip Airfoil	c_{tip}	7.22 ft	2.2 m

The provided coordinates for the B-29 airfoil profiles do not perfectly align between the top and bottom surfaces, making it challenging to calculate the mean camber line $\bar{z}$. (In other words, the x coordinates do not perfectly match between the upper and lower surfaces, so directly averaging the y coordinates at each x location is not possible.) To get around this, I fitted a smooth cubic spline curve to each surface - averaging the spline curves provides an approximation of the mean camber line $\bar{z}$, even in regions where the original coordinates do not align.

This method works well for plotting the airfoil shapes, as shown in Figure 1 as the spline curves provide a continuous representation of the surfaces.

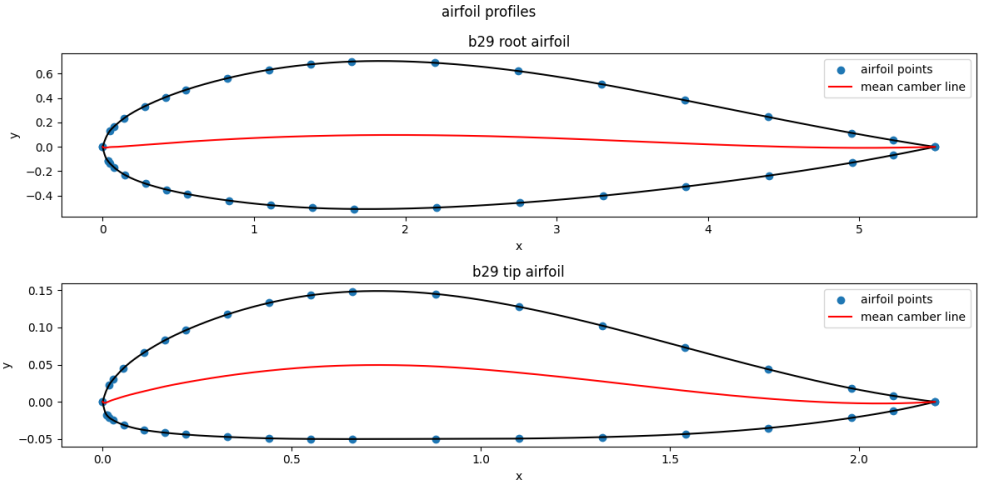

Figure 1: Cubic spline interpolation of the B-29 root and tip airfoil upper and lower surfaces, with the averaged splines approximating the mean camber line $\bar{z}$.

Air properties at cruising altitude were estimated using XFLR5; you can take a peek in Figure 2. These properties were used for the calculation of forces and nondimensional parameters such as the Reynolds number.

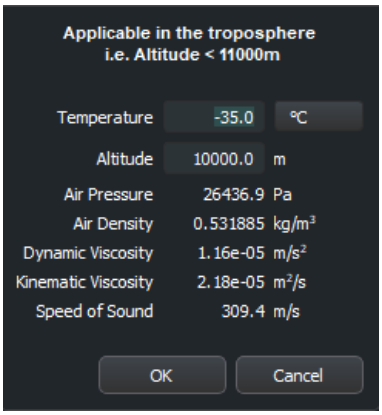

Figure 2: Fluid properties for $z = 10$ km and $T = 35°\text{C}$.

The Reynolds number of the flow passing the root airfoil at cruising speed is:

$$\text{Re}_c = \frac{V_{\text{cruise}} c_{\text{root}}}{\nu} = \frac{(98.35 \text{ m/s})(5.5 \text{ m})}{2.18\text{e-}5 \text{ m}^2/\text{s}} = 2.5\text{e}7$$

3 Thin Airfoil Theory

Thin airfoil theory provides a powerful analytical approach to determine the fundamental lift and moment characteristics of cambered airfoils. By using the solution to the canonical cambered thin airfoil problem, we can calculate key parameters such as the lift curve slope, zero-lift angle, and section lift coefficient vs. angle of attack.

The cambered thin airfoil problem requires finding the vortex-sheet strength $\gamma(x)$ from the integral equation:

$$\frac{1}{2\pi}\int_0^c \frac{\gamma(\xi)}{\xi - x}\,d\xi = V_\infty\left[\alpha - \frac{d\bar{z}}{dx}\right]$$

This equation can be rewritten in terms of the angle θ as:

$$\frac{1}{2\pi}\int_0^\pi \frac{\gamma(\theta)\sin(\theta)}{\cos(\theta) - \cos(\varphi)}\,d\theta = V_\infty\left[\alpha - \frac{d\bar{z}}{dx}\right]$$

The solution for $\gamma(\theta)$ is found by representing it as a Fourier sine series (this is only a solution if we assume that the mean camber line is a streamline):

$$\gamma(\theta) = 2V_\infty\left(A_0\frac{1+\cos(\theta)}{\sin(\theta)} + \sum_{n=1}^{\infty} A_n\sin(n\theta)\right)$$

Some additional algebraic manipulation yields:

$$\frac{1}{\pi}\int_0^\pi \frac{A_0(1+\cos(\theta))}{\cos(\theta) - \cos(\varphi)}\,d\theta + \int_0^\pi \sum_{n=1}^{\infty}\frac{A_n\sin(n\theta)\sin(\theta)}{\cos(\theta) - \cos(\varphi)}\,d\theta = \alpha - \frac{d\bar{z}}{dx}$$

and using a bunch of trigonometric identities, we get that:

$$\frac{d\bar{z}}{dx} = \alpha - A_0 + \sum_{n=1}^{\infty} A_n\cos(n\varphi)$$

This equation must be satisfied at every chordwise location x along the airfoil. At a given chordwise station x, the left-hand side of the equation is known, and the corresponding angle φ is determined by the transformation $x = 0.5c(1 - \cos(\varphi))$. (It's also important to note that this equation could equivalently be written in terms of θ instead of ϕ, as both angles correspond to a specific chordwise station on the airfoil. However, when both variables appear together in an integrand, they must be carefully distinguished from each other.)

When we integrate this equation over the interval $\Omega = [0, \pi]$, we get:

$$A_0 = \alpha - \frac{1}{\pi}\int_0^\pi \frac{d\bar{z}}{dx}\,d\varphi$$

and the remaining A_n can be found using the following equation (I only bothered finding A_1 and A_2 for reasons that will become clear soon.)

$$A_n = \frac{2}{\pi}\int_0^\pi \frac{d\bar{z}}{dx}(\cos(n\varphi))d\varphi$$

My expression for $\bar{z}$, as defined in my code, is a pain to differentiate. This is because a cubic spline is a

piecewise function, meaning it is defined by different cubic polynomial pieces over different intervals or segments. This is a headache to deal with when using a symbolic computation library like `sympy`. To get around THAT, I fitted that spline to a 7th-degree polynomial.

$$\bar{z} = -0.448x^7 + 1.641x^6 - 2.484x^5 + 2.110x^4 - 0.971x^3 + 0.064x^2 + 0.091x - 0.001$$

$$\begin{aligned}\frac{d\bar{z}}{dx} = &-0.049(1-\cos(\varphi))^6 + 0.308(1-\cos(\varphi))^5 - 0.776(1-\cos(\varphi))^4 \\ &+ 1.055(1-\cos(\varphi))^3 - 0.729(1-\cos(\varphi))^2 - 0.064(1-\cos(\varphi)) + 0.154\end{aligned}$$

`sympy` did not have a fun time integrating that. Despite significant efforts to optimize the code, it still tool approximately six minutes for the symbolic integration to complete and obtain the values of A_1 and A_2. To reduce the computational workload and enhance the efficiency of future runs, I decided to store the calculated values as `numpy` objects, which eliminates the need to recalculate these coefficients every time the script is executed.

Here are some results!

$$A_0 - \alpha = -0.018 \qquad A_1 = 0.046 \qquad A_2 = 0.074$$

The section lift coefficient as a function of angle of attack is written as follows:

$$\begin{aligned}c_l(\alpha) &= 2\pi\left[\alpha + \frac{1}{\pi}\int_0^\pi \frac{d\bar{z}}{dx}(\cos(\varphi) - 1)\, d\varphi\right] \\ &= \pi\left[2\alpha + \frac{2}{\pi}\int_0^\pi \frac{d\bar{z}}{dx}\cos(\varphi)\, d\varphi - \frac{2}{\pi}\int_0^\pi \frac{d\bar{z}}{dx}\, d\varphi\right] \\ &= \pi[2\alpha + A_1 + 2(A_0 - \alpha)] \\ &\approx 2\pi\alpha + 0.01\pi\end{aligned}$$

The lift-curve slope is 2π, as expected by the theory - my script spits out 6.283185... (it's stored under the name `b29_root.dCl_dalpha`). The zero-lift angle of attack $\alpha_{L=0}$ turns out to be -0.0051 radians, or -0.29 degrees.

The section moment coefficient for a cambered airfoil is only dependent on A_0, A_1, and A_2, so I feel justified in my decision to stop integrating there... if I was interested in finding the chordwise pressure distribution, I'd definitely have to calculate more.

$$c_{M|LE} = -\frac{\pi}{2}\left[A_0 + A_1 - \frac{A_2}{2}\right] = -\frac{c_l}{4} + \frac{\pi}{4}(A_2 - A_1)$$

$c_l(\alpha)$ and $c_{m|LE}(\alpha)$ are plotted in Figure 3. I'm also plotting $F_l(\alpha)$ in Figure 4, with the maximum takeoff weight also plotted.

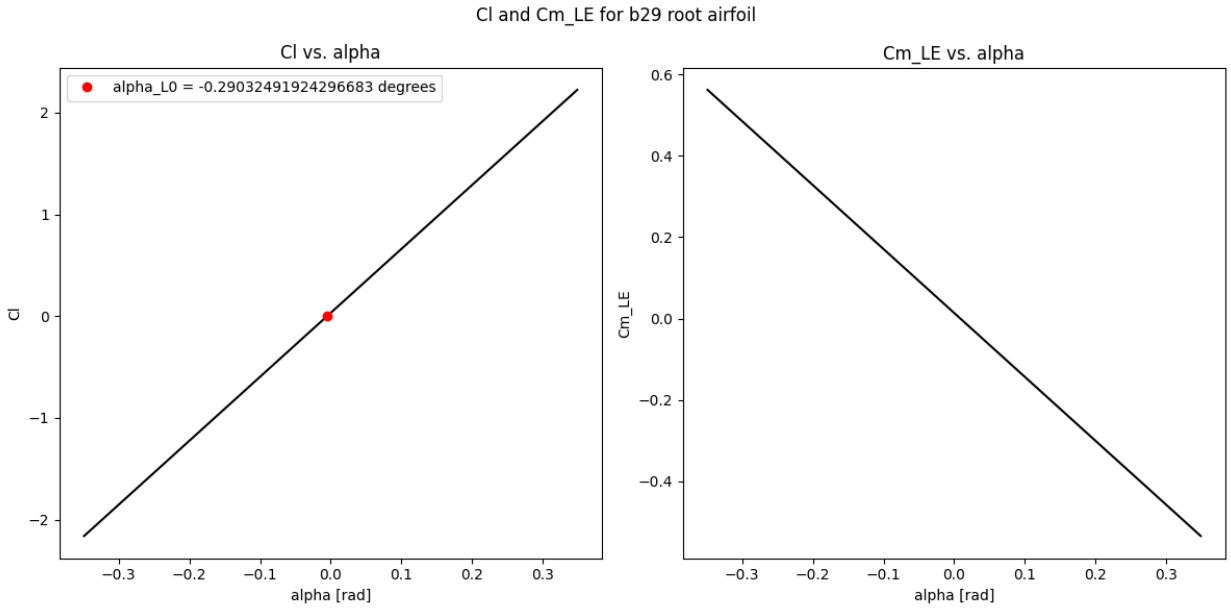

Figure 3: $c_l(\alpha)$ and $c_{m|LE}(\alpha)$.

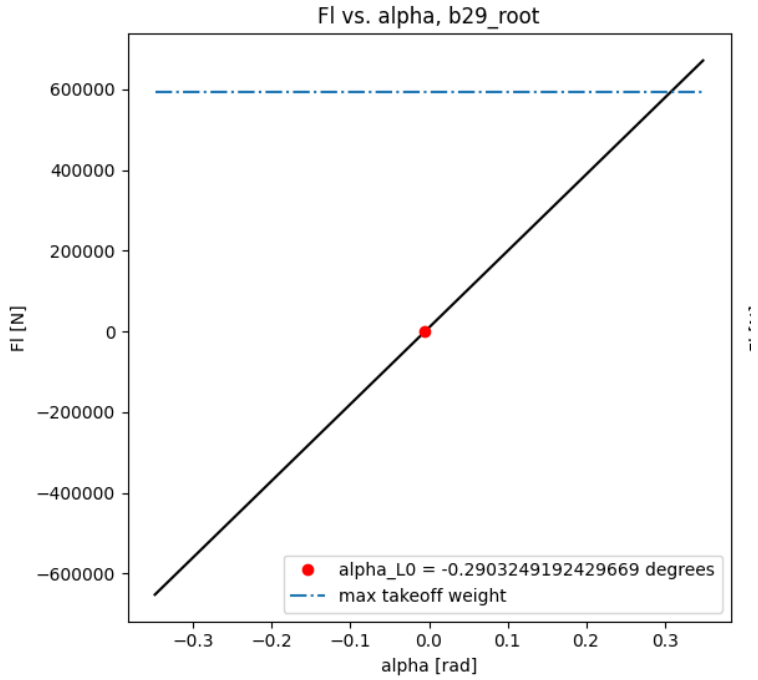

Figure 4: $F_l(\alpha)$ with maximum takeoff weight also plotted.

4 Estimating Lift Force using Finite Wing Theory

Finite wing theory accounts for the real-world effects that arise due to the finite span of wings, in contrast to the idealized assumptions of infinite wing theory. It acknowledges the formation of wingtip vortices, which are swirling flows generated near the wing tips due to the spanwise pressure differential. These vortices induce a downward deflection of the airflow behind the wing, known as downwash, altering the effective angle of attack experienced by different sections along the wingspan.

As a result, the lift distribution becomes non-uniform across the span, deviating from the idealized two-dimensional case. This non-uniform lift distribution, coupled with the induced drag caused by the wingtip vortices, impacts the overall aerodynamic performance of the aircraft. Finite wing theory provides a more realistic representation of the complex flow phenomena associated with finite-span wings, enabling more realistic predictions of lift, drag, and other aerodynamic characteristics.

For a finite wing of arbitrary shape and airfoil, we can calculate the coefficient of lift using the following equation:[1]

$$C_L = \frac{2}{V_\infty S} \int_\pi^0 \left[(2bV_\infty) \sum_{n=1}^{\infty} A_n \sin(n\theta) \right] \left[\frac{b}{2} (-\sin(\theta)\, d\theta) \right] = \pi A_1 (\mathrm{AR})$$

As expected, the finite wing estimate for the coefficient of lift C_L is lower than the section lift coefficient from thin airfoil theory c_l, as shown in Figure 5. This can be attributed to a few key points:

- On a finite wing, the high pressure air below the wing flows around the wingtip towards the low pressure region above the wing, creating wingtip vortices. These vortices induce a downwash behind the wing, effectively reducing the angle of attack and lift.
- Thin airfoil theory assumes an elliptical spanwise lift distribution for minimum induced drag. However, real wings have a non-elliptical lift distribution, leading to higher induced drag and lower effective lift.

I've also zoomed in on a characteristic angle of attack (0.15 rad) in Figure 6. Cruising speed was used for the force calculation, so that angle of attack might be uncharacteristically (aha!) high, but it's just a case study, so no harm no foul.

[1] Obviously, I'm brushing over a lot of the background surrounding the fundamental monoplane equation, but it's 4:37 AM and I'm starting to see TV static. -BA

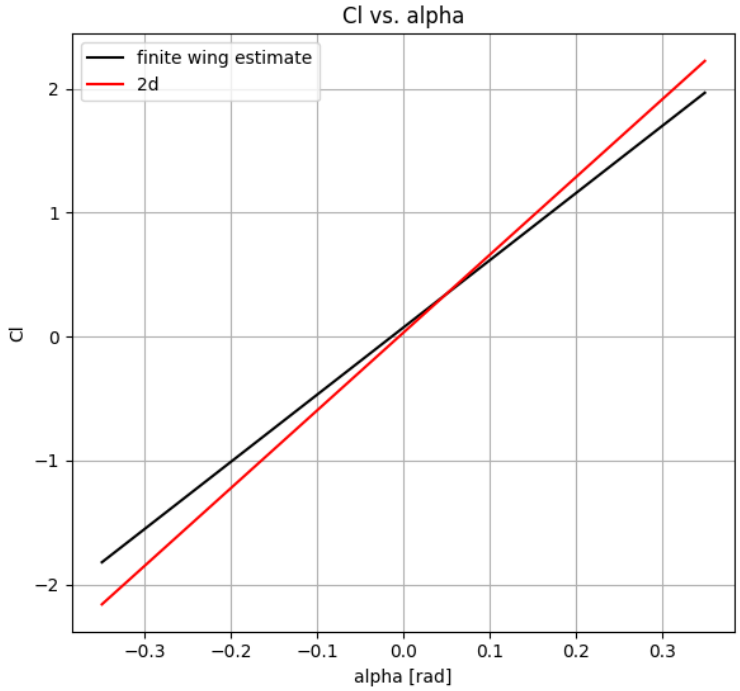

Figure 5: $C_L(\alpha)$ for the wing compared with $c_l(\alpha)$ for the root airfoil section.

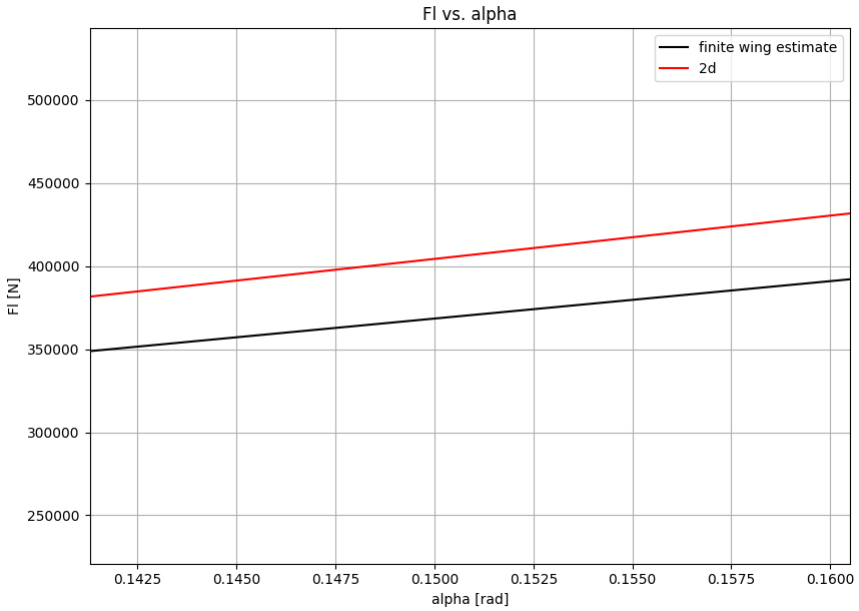

Figure 6: $F_L(\alpha)$ for the wing compared with $F_l(\alpha)$ for the root airfoil section, for $V = V_{\text{cruise}}$ and $\alpha = 0.15$ rad.

5 Drags (Two Different Ones)

Induced drag is a type of drag that arises due to the production of lift by a finite wing. It's caused by the wingtip vortices that are created as a result of the pressure difference between the lower and upper surfaces of the wing. The induced drag coefficient depends on the lift coefficient squared, aspect ratio, and a span efficiency factor related to the wing planform and lift distribution.

$$C_{D,\text{induced}} = \frac{C_L^2}{\pi(\text{AR})}(1+\delta)$$

where:

$$\delta = \sum_{n=2}^{\infty} n\left(\frac{A_n}{A_1}\right)^2$$

Figure 7 shows the induced drag plotted against various angles of attack.

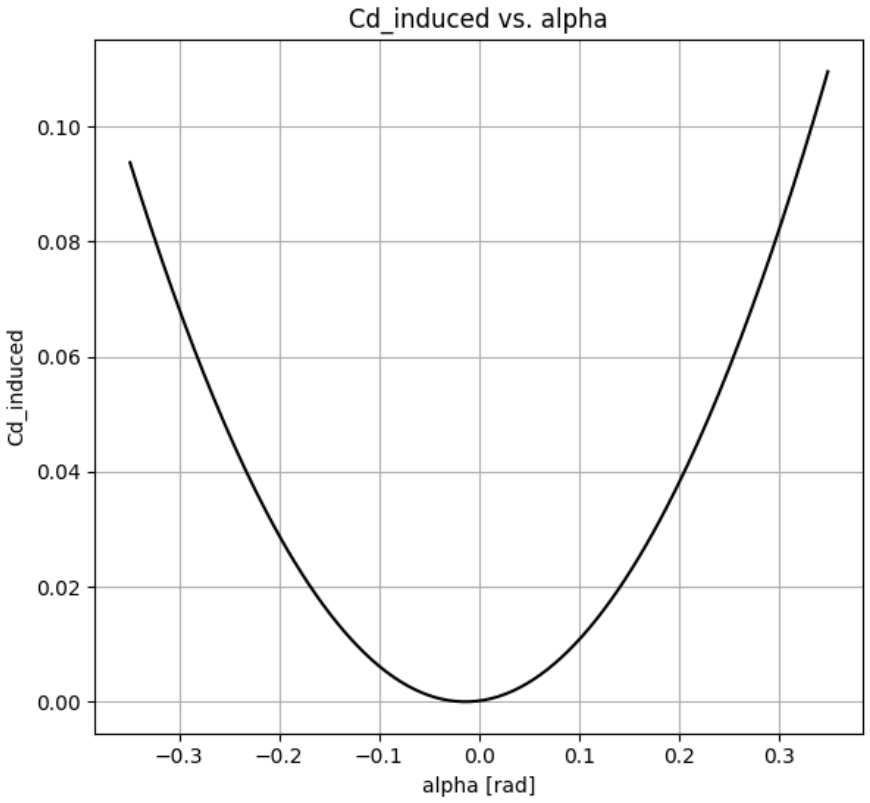

Figure 7: $C_{D,\text{induced}}(\alpha)$. Note that $C_{D,\text{induced}}$ is several degrees of magnitude smaller than C_L for positive angles of attack.

Skin friction drag, on the other hand, is the component of aerodynamic drag caused by the shear stress acting on the surface of an object due to viscous effects in the fluid flow. I used strip theory to calculate skin drag - dividing the surface into streamwise strips and integrating the local skin friction coefficients over each strip.

I divided the wing span into 100 sections using a linearly spaced array of points along the semi-span. The chord length at each spanwise section is calculated based off the root and tip airfoil chord lengths, assuming a linear taper from root to tip. Then, a "critical length" l_{crit} is calculated based on the critical Reynolds number $\text{Re}_{\text{crit}} = 3 \times 10^5$. This length is used to determine the transition from laminar to turbulent flow.

The turbulent local skin friction coefficient is calculated using the Blasius formula for turbulent flow over a flat plate:

$$C_{f,\text{turbulent}} = \frac{0.027}{\text{Re}_x^{1/7}}$$

and the laminar local skin friction coefficient is calculated using the corresponding formula for laminar flow over a flat plate:

$$C_{f,\text{laminar}} = \frac{0.664}{\sqrt{\text{Re}_x}}$$

An "overlap" term is calculated to account for the transition between laminar and turbulent flow; this term is subtracted from the turbulent drag later to avoid double-counting.

The total skin friction drag is calculated by summing the aforementioned components and multiplying by a factor of 2 - this corrective factor accounts for the drag contribution from both the upper and lower surfaces of the wing. My script spat out:[2]

$$C_{d,\text{viscous}} = 0.020 \qquad F_{d,\text{viscous}} = 6213 \text{ N}$$

Figures 8 and 9 show plots of the total drag coefficient C_D against α and C_L, respectively. (Figure 9 also has the lift-to-drag ratio plotted against α.)

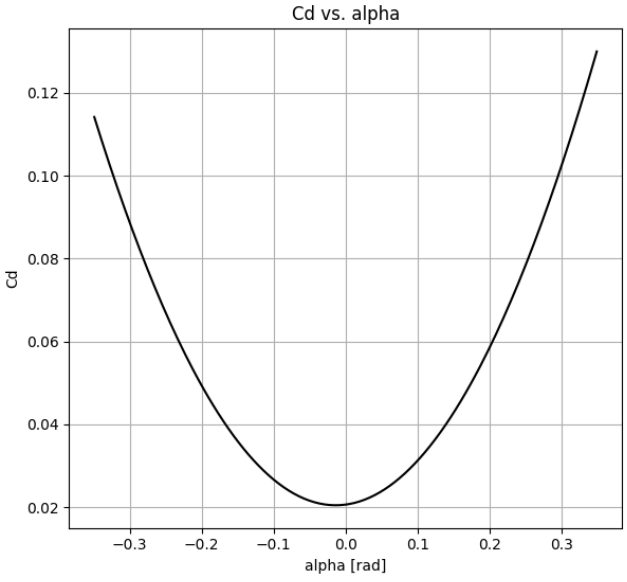

Figure 8: $C_D(\alpha) = C_{D,\text{induced}}(\alpha) + C_{D,\text{viscous}}$.

[2]Off my intuition, skin friction coefficient should be relatively constant for small angles of attack. There's probably a more realistic approximation for skin friction that is dependent on angle of attack, but this constant value should suffice for this use case. -BA

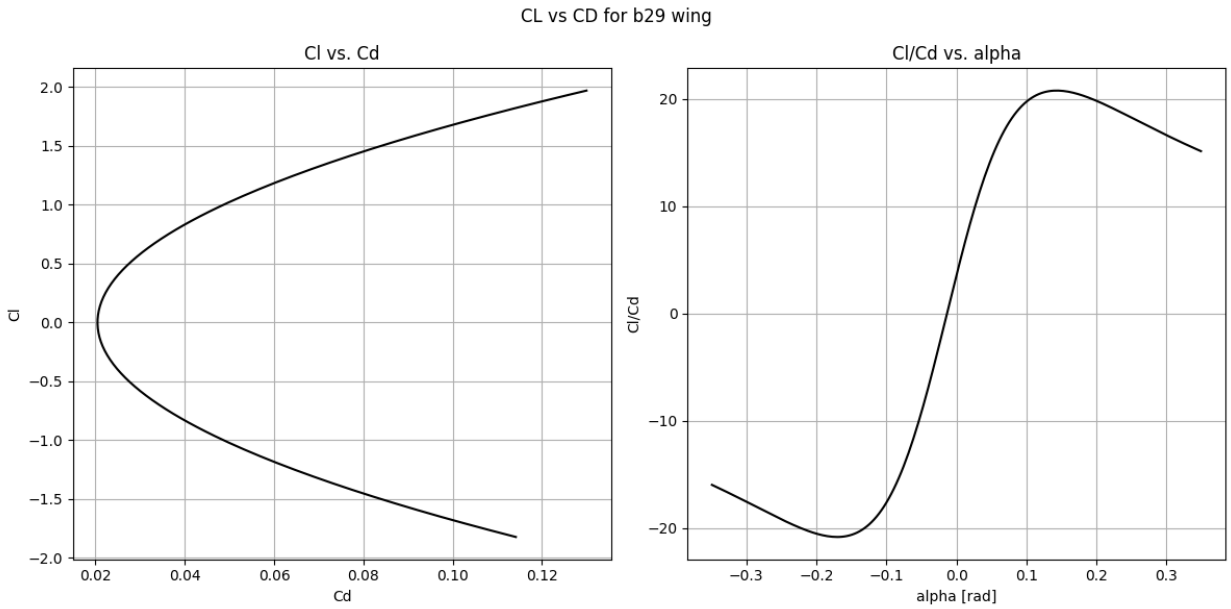

Figure 9: C_L plotted against C_D, and lift-to-drag ratio C_L/C_D plotted against α.

6 Computational Validation Using XFLR5

XFLR5 is a free and open-source software tool for analyzing airfoils, wings, and aircraft designs operating at low Reynolds numbers. It incorporates the XFoil analysis code developed by Mark Drela at MIT, which allows for direct and inverse analysis of airfoils, but unlike XFoil, it provides a graphical user interface.

XFLR5 can perform various types of analyses, including viscous and inviscid flow analyses, stability analyses, and flight simulations. It also supports batch analyses, scripting capabilities, and optimization modules for airfoil and wing design.

To perform a wing analysis, I first constructed the root and tip airfoils in the "Direct Foil Design" tool. I had a few issues with importing `.dat` files from Airfoil Tools because XFLR5 heavily prefers when you input a set of points starting at the trailing edge, going to the leading edge, then back (this is apparently known as the Selig format).

I ran an analysis of the root airfoil at $\text{Re}_c = 2.5\text{e}7$ to see how close the thin airfoil theory calculations were (see Figure 9). The zero-lift angle of attack is larger in magnitude (-0.29° according to thin airfoil theory vs. -1.2° according to XFLR5), but the numbers are not unreasonable.

The moment coefficients, however, gave me pause. While the predictions from thin airfoil theory seem to be valid for higher angles of attack, near 0, they seem wildly off.

I'm generally pretty wary of the validity of my thin airfoil theory calculations - that 7th-degree polynomial fit might have sacrificed some of the detail of the mean camber line, making the foil more "symmetric". Oh well, you live and you learn.

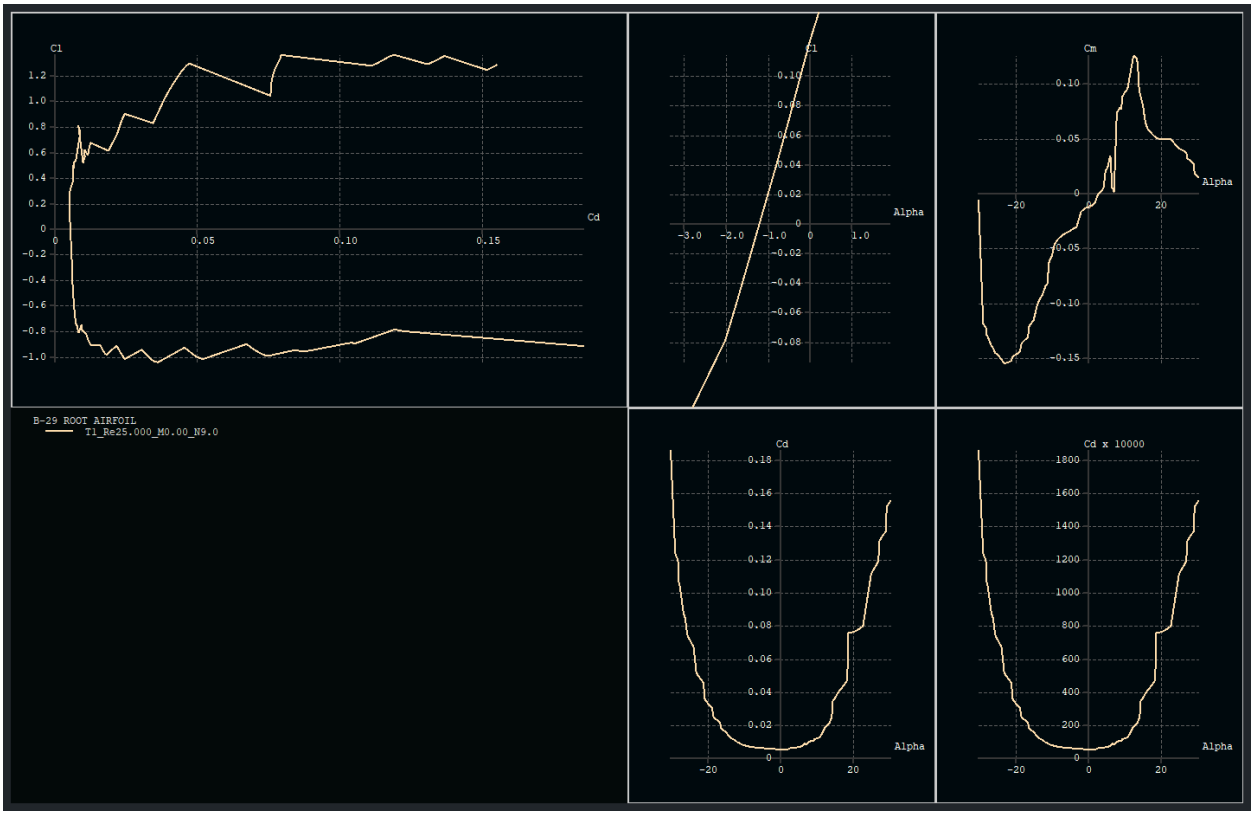

Figure 10: Various lift and drag polars for the B-29 root airfoil, at a Reynolds number of 2.5e7.

Onto the wing!

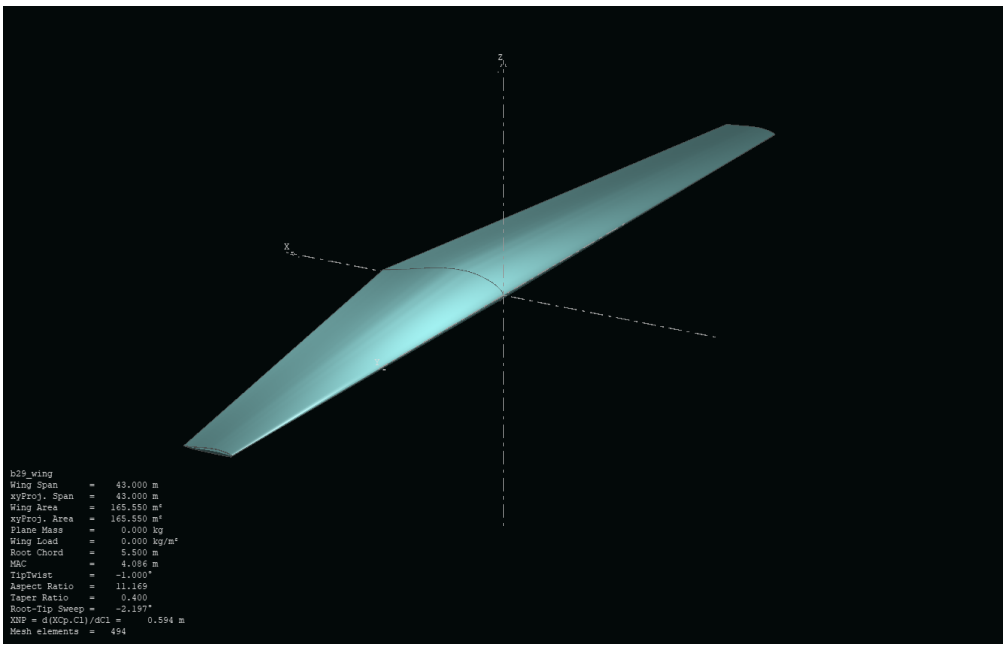

Figure 11: Wing, as modeled in XFLR5.

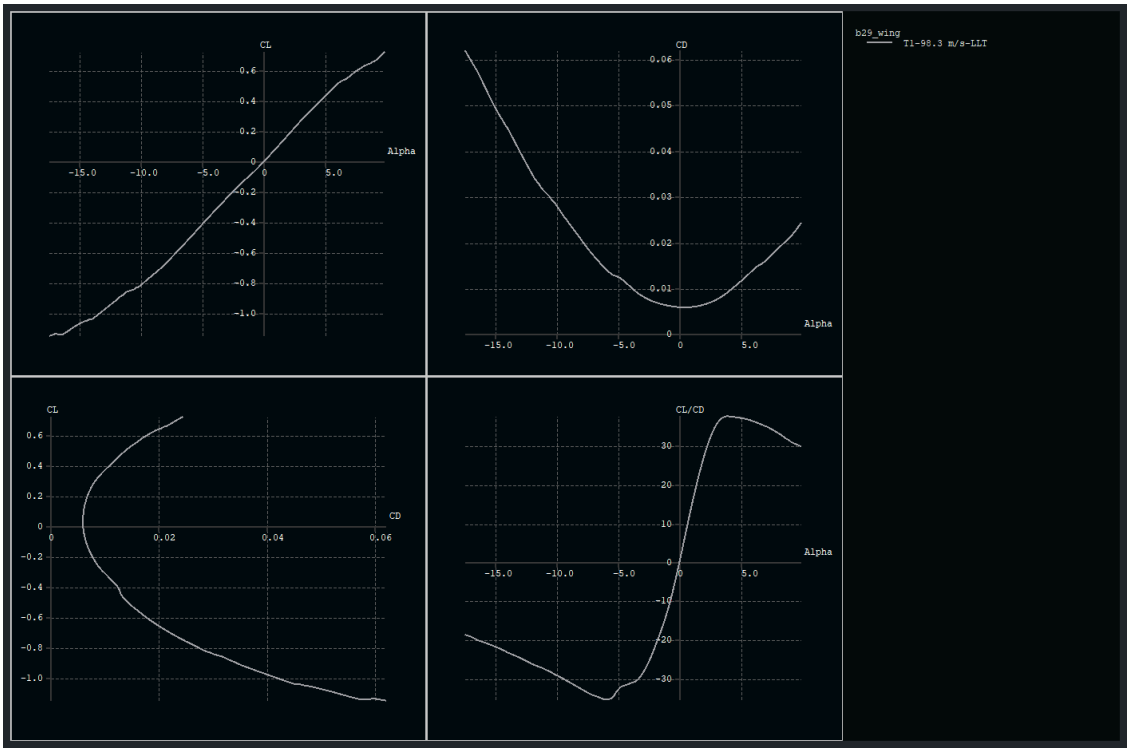

Figure 12: Plots of $C_L(\alpha)$, $C_D(\alpha)$, C_L vs. C_D, and L/D vs. α.

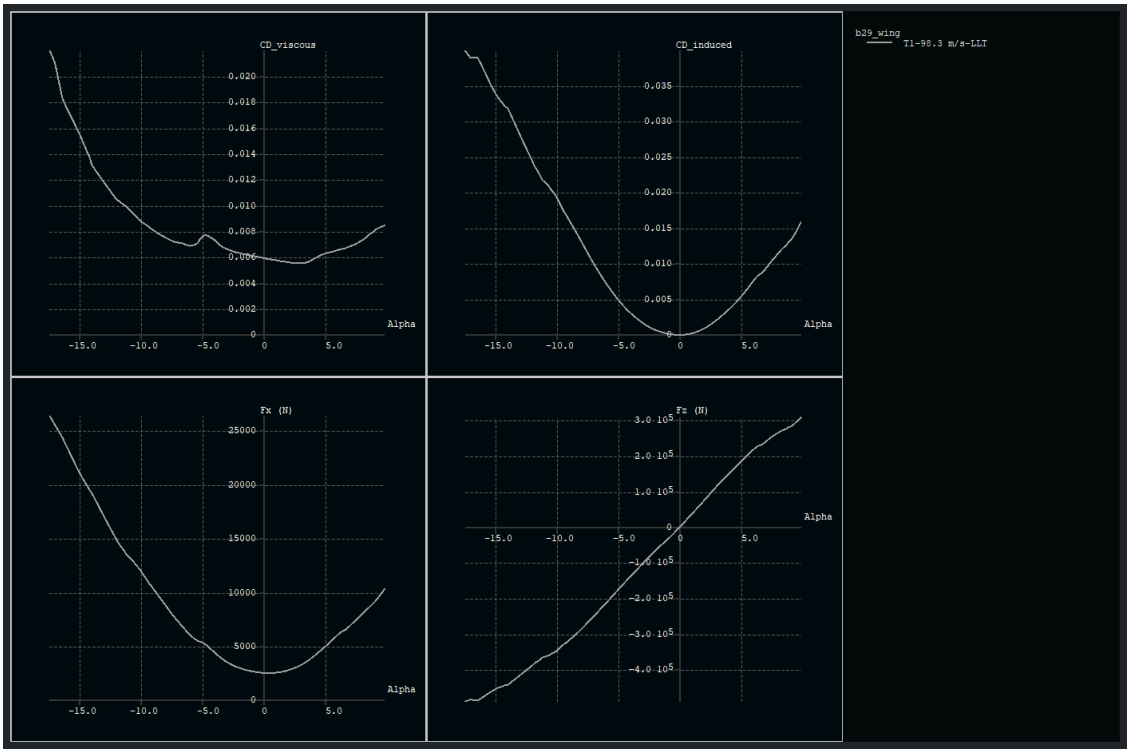

Figure 13: $C_{D,\text{viscous}}(\alpha), C_{D,\text{induced}}(\alpha), F_D(\alpha)$, and $F_L(\alpha)$

The finite wing calculations seemed to yield better predictions than the 2D hand calculations. The zero-lift angle of attack seems to be more accurate here, around -1°...

My theoretical predictions for induced drag look spot-on, though. My calculations for viscous drag seemed to overestimate it by a factor of 3, but the assumption that the drag was relatively constant for small angles of attack seems to be valid. The viscous drag dominates for small angles of attack, but once outside the window of $\theta = [-5, 5]$ degrees, the induced drag has a higher effect.

The stall speed can be calculated using the following equation:

$$V_{\text{stall}} = \sqrt{\frac{2W}{\rho S C_L}}$$

XFLR5 LLM wing analysis will not converge for angles of attack above 9.8°, so I'm going to use an estimate based off the 2D $c_l(\alpha)$. As seen in Figure 14, the airfoil stalls at $\alpha \approx 18°$, with a $c_l = 1.29$.

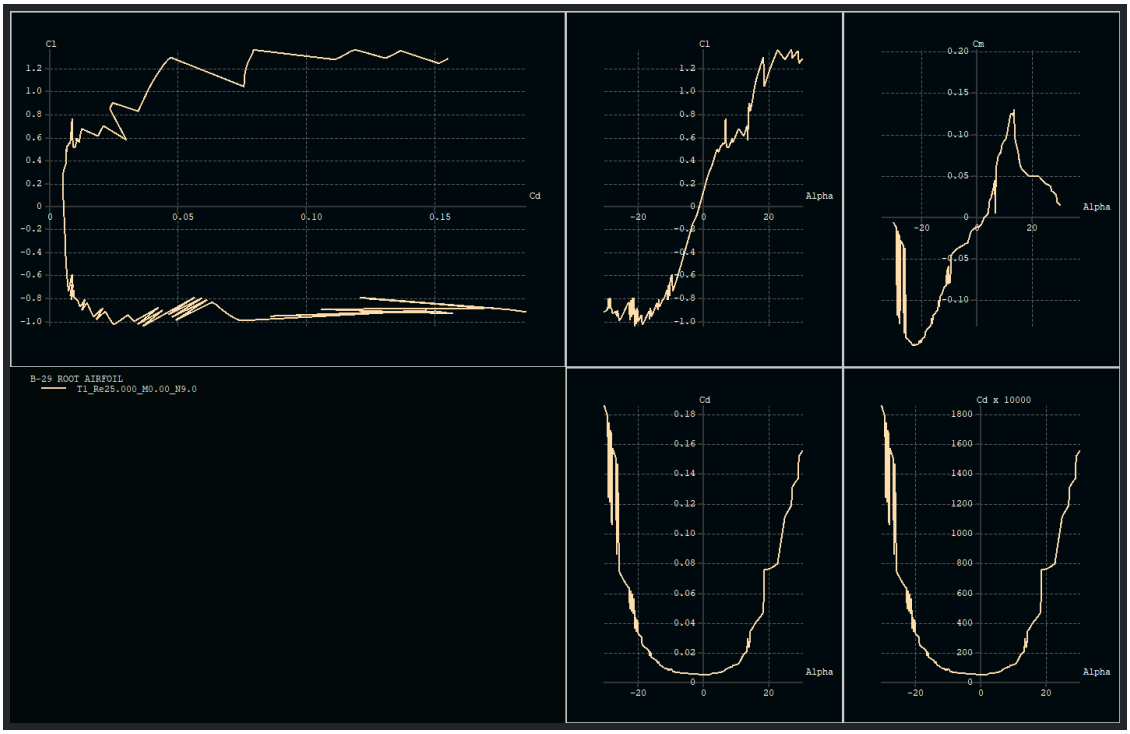

Figure 14: $C_L(\alpha)$, for an expanded domain than in Figure 10.

I think the coefficient of lift there acts as a good ceiling for stall prediction.

$$V_{\text{stall}} = \sqrt{\frac{2(593837.37 \text{ N})}{(0.532 \text{ kg/m}^3)(161.3 \text{ m}^2)(1.29)}} = 103.58 \text{ m/s}$$

I'm not particularly concerned about the magnitude of the stall speed; the documented maximum speed of the B-29 is 357 mph (or 159.6 m/s), implying that there may be other mechanisms in place to delay stall. In fact, the B-29 Superfortress employed several mechanisms to delay stall and maintain lift at high speeds.

Further research revealed that the B-29 wings were equipped with leading edge slats that extended at high angles of attack. These slats energized the airflow over the wing's leading edge, delaying flow separation and stall.

Additionally, the B-29 had special dive recovery flaps on the wings to counteract compressibility effects and maintain lift at high speeds, effectively delaying stall. This was a solution developed by NACA's John Stack to the "tuck under" problem faced by the P-38 Lightning at high speeds.

A References

1. J. W. Mitchell, A. T. McDonald, and R. W. Fox, *Fox and McDonald's Introduction to Fluid Mechanics, 10th ed.* Hoboken, NJ, USA: John Wiley & Sons, 2020.

2. Airfoil Tools, "Airfoil Tools," Available: http://airfoiltools.com/

3. National Museum of the U.S. Air Force, "Boeing B-29 Superfortress," [Online].

4. Nuclear Companion, "Boeing B-29 Superfortress Specifications (1950)," [Online]. Available: https://nuclearcompanion.com/data/boeing-b-29-superfortress-specifications-1950/

5. xflr5, "xflr5," [Online]. Available: https://www.xflr5.tech/xflr5.htm

6. G. A. Flandro, H. M. McMahon, and R. L. Roach, *Basic Aerodynamics: Incompressible Flow*, Cambridge Aerospace Series. Cambridge, U.K.: Cambridge Univ. Press, 2011. [Online].

7. J. D. Anderson, *Fundamentals of Aerodynamics*. New York, NY, USA: McGraw-Hill Education, 2016. [Online]. Available: https://books.google.com/books?id=D1ZojgEACAAJ

8. F. M. White and J. Majdalani, *Viscous Fluid Flow*, 4th ed. New York, NY, USA: McGraw-Hill Education, 2021.

B Calculations

Most of the theory ended up in the body of the report already. My code can be found at https://github.com/destrospooder/b29_analysis.

C Acknowledgements

Thanks to Khushant Khurana for sending me a LaTeX title page template he found that I liked.

Thanks to Sohaib Bhatti for caring so much about the environment.

Thanks to Ahmed Hassan for being the best Ahmed Hassan one could be.

Thanks to the Coca-Cola Company for making crappy bottles. Just spilled half a bottle of Diet Coke on the floor. What a day.

Thanks to Tanner Wootton for making me remember I have a Beyblade collection.

Thanks to Sonam Okuda for sending me (unrelated to ME422) bad graphs.

Thanks to the International Bureau of Weights and Measures for coordinating the International System of Units.

Thanks to Eunkyu (Q) Kim for suggesting I stop writing this report and play "Dungeon Fighter Online" instead. (I don't know what that is.)

Thanks to some random YouTuber Sid G for teaching me XFLR5.

Thanks to the Staten Island Ferry. Particularly the really old, shit boats.

Thanks to the mosquito in my room for keeping me company while writing this paper.